SCIENCE CHINA
Information Sciences

• MOOP •

November 2018, Vol. 61 114101:1–114101:3
https://doi.org/10.1007/s11432-018-9518-3

# Adaptive narrow band MultiFLIP for efficient two-phase liquid simulation

Luan LYU[1†], Xiaohua REN[1*†], Wei CAO[1], Jian ZHU[4] & Enhua WU[1,2,3]

[1]*Faculty of Science and Technology, University of Macau, Macao* 999078*, China;*
[2]*State Key Laboratory of Computer Science, Institute of Software, Chinese Academy of Sciences, Beijing* 100190*, China;*
[3]*Zhuhai-UM Science and Technology Research Institute, Zhuhai* 519000*, China;*
[4]*School of Computer Science, Guangdong University of Technology, Guangzhou* 510000*, China*

Received 9 April 2018/Accepted 29 June 2018/Published online 28 September 2018

**Citation** Lyu L, Ren X H, Cao W, et al. Adaptive narrow band MultiFLIP for efficient two-phase liquid simulation. Sci China Inf Sci, 2018, 61(11): 114101, https://doi.org/10.1007/s11432-018-9518-3

Liquid-gas interactions produce many interesting phenomena such as droplets, bubbles, and the "glugging" effect of water pouring. Reproducing those phenomena, however, are difficult problems in both the computational physics and computer graphics communities. In order to simulate these two-phase phenomena, Boyd and Bridson [1] proposed the MultiFLIP method, which is an extension of the fluid implicit particle (FLIP) method introduced by Zhu and Bridson [2] and preserves all its good properties such as excellent conservation of energy with little dissipation.

Since both gas and liquid phases are involved, MultiFLIP has two challenges: first, a total number of $8n^3$ gas and liquid particles are required to fill the gas and liquid volumes; second, a variable coefficient Poisson equation needs to be solved on the entire domain. The two challenges significantly limit the scalability of MultiFLIP. In order to address the challenges, we present OctNB-MutliFLIP. Our method incorporate narrow band and octree techniques to MultiFLIP, which were respectively proposed by Ferstl et al. [3] and Losasso et al. [4] for one-phase liquid simulations.

*MultiFLIP.* We briefly introduce MultiFLIP [1], which is based on the inviscid, incompressible Navier-Stokes equations (see [5]),

$$\partial_t \boldsymbol{u} + (\boldsymbol{u}\cdot\nabla)\boldsymbol{u} = -\frac{1}{\rho}\nabla p + \frac{1}{\rho}\boldsymbol{g}, \quad \nabla\cdot\boldsymbol{u} = 0, \quad (1)$$

where $\boldsymbol{u}$ is velocity, $p$ is pressure, $\rho$ is density, and $\boldsymbol{g}$ is external force such as gravity.

MulitFLIP employs two kinds of particles, one for gas and the other for liquid, and also two velocity fields, $\boldsymbol{u}_g$ for gas and $\boldsymbol{u}_l$ for liquid. MultiFLIP adds three steps to FLIP. The first one is to construct the gas-liquid interface from particles. This step first constructs a level-set function and then re-initialize it by the fast marching method. The second one is to separate gas and liquid particles mixing at the gas-liquid interface by bumping and re-sampling particles. The last one is to preserve sub-grid bubbles and droplets by handling escaped particles.

Different from FLIP to solve a constant Poisson equation, MultiFLIP solves a variable coefficient Poisson equation

$$\nabla\cdot\frac{1}{\rho}\nabla p = \nabla\cdot(\boldsymbol{u}_g^* + \boldsymbol{u}_l^*), \quad (2a)$$

$$\boldsymbol{u}_g = \boldsymbol{u}_g^* - \left(\frac{1}{\rho}\nabla p\right)\Big|_g, \quad (2b)$$

$$\boldsymbol{u}_l = \boldsymbol{u}_l^* - \left(\frac{1}{\rho}\nabla p\right)\Big|_l, \quad (2c)$$

where $(\frac{1}{\rho}\nabla p)|_g$, $(\frac{1}{\rho}\nabla p)|_l$ denote the restriction of

* Corresponding author (email: xiaohua_ren@126.com)
† Lyu L and Ren X H have the same contribution to this work.

 

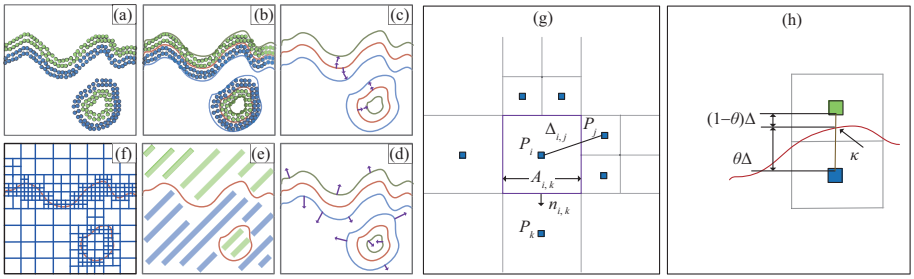


| Case name | Resolution | Method | Average # particles (million) | | | Average time/timestep (s) | | | Mem. (MB) |
|---|---|---|---|---|---|---|---|---|---|
| | | | Gas | Liquid | Total | Projection | Rest | Total | |
| Tension | $128^3$ | MultiFLIP | 18.72 | 1.92 | 20.65 | 7.8 | 28.2 | 36.0 | 4932 |
| | | Ours | 0.47 | 0.42 | 0.89 | 2.3 | 5.5 | 7.8 | 954 |
| Dambreak | 128 × 128 × 64 | MultiFLIP | 9.2 | 2.84 | 12.04 | 14.4 | 21.0 | 35.4 | 2648 |
| | | Ours | 0.38 | 0.38 | 0.76 | 2.6 | 4.7 | 7.3 | 537 |
| Box glugging | 64 × 256 × 64 | MultiFLIP | 9.11 | 1.83 | 10.90 | 12.8 | 19.7 | 32.5 | 2426 |
| | | Ours | 0.47 | 0.33 | 0.80 | 3.4 | 5.1 | 8.5 | 557 |
| Bubble | 64 × 128 × 64 | MultiFLIP | 1.44 | 4.32 | 5.75 | 5.4 | 10.4 | 15.8 | 1249 |
| | | Ours | 0.20 | 0.25 | 0.45 | 1.7 | 2.9 | 4.6 | 282 |
| Bubble | 128 × 256 × 128 | MultiFLIP | – | – | – | – | – | – | – |
| | | Ours | 0.69 | 0.85 | 1.55 | 10.8 | 14.1 | 24.9 | 1963 |
| Sandglass | 128 × 256 × 128 | MultiFLIP | – | – | – | – | – | – | – |
| | | Ours | 0.75 | 0.90 | 1.65 | 15.6 | 16.1 | 31.8 | 2040 |

(i)

**Figure 1** (Color online) (a)–(e) are the substeps of 2D gas-liquid interface tracking in OctNB-MultiFLIP; (f) shows the constructed octree with fine grid cells near the interface; (g) discretization of the variable coefficient Poisson equation on a quadtree; (h) computation of $\theta$ for two cells crossed by the interface (red colored curve), where $\Delta$ is the distance between the two cells and $\kappa$ is the curvature at the interface; (i) shows comparisons of particle number and run-time of OcNB-MultiFLIP to MultiFLIP for different cases.

$\frac{1}{\rho}\nabla p$ to the gas and liquid domains, respectively. In this step, because there is a sharp jump in density and pressure gradient and, when surface tension is present, pressure at the gas-liquid interface, MultiFLIP uses the ghost fluid method [6] to capture these discontinuities.

*Octree-based narrow band MultiFLIP* (*OctNB-MultiFLIP*). The key ingredients of our method are two adaptive techniques adapted to MultiFLIP. First, we extend the narrow band method of Ferstl et al. [3] (hereafter referred to as NB-FLIP) to MultiFLIP. Second, we propose to discretize the variable coefficient Poisson on an octree structure with refined grid cells near the gas-liquid interface.

*Narrow band MultiFLIP*. We need three steps: interface tracking, grid-particle coupling and particle resampling, to turn MultiFLIP into OctNB-MultiFLIP. In the following, we will dive into the details of those steps.

Step 1: interface tracking. In our method, we use two narrow bands: one for the gas phase and the other for the liquid phase. It is found that we can uniquely determine the gas and liquid phases without the additional level set function as used in NB-FLIP.

Figure 1 shows the substeps of our interface tracking. First, we initialize a level-set function $\phi$ (Figure 1(b)) from the two bands of gas (green circles) and liquid (blue circles) particles as shown in Figure 1(a). Then, we re-initialize the function on the bands by fast marching method (Figure 1(c)). We use the faster flood-fill algorithm to initialize the function as shown in Figure 1(d) to determine whether those regions are occupied by the liquid or gas. Finally, we obtain the final level-set function $\phi$, by which we can uniquely identify the gas (green color) and liquid (blue color) phases and the interface (red color) as shown in Figure 1(e).

Step 2: grid-particle coupling. After advecting the gas and liquid particles, we map them to grid and obtain the gas and liquid velocity: $\boldsymbol{u}_g^p$ and $\boldsymbol{u}_l^p$. Similar to the level set function defined above, those two velocity fields on the particle-free regions have not been initialized. To address this issue, we employ two additional grid velocity $\boldsymbol{u}_g$ and $\boldsymbol{u}_l$ to track the velocities on the particle-free domains, each of which is treated in the same way as NB-FLIP. That is, we first advect $\boldsymbol{u}_g$ ($\boldsymbol{u}_l$) on the entire domain by performing a semi-Lagrangian advection step, which yields advected grid velocity $\boldsymbol{u}_g'$ (resp. $\boldsymbol{u}_l'$). Then, we combine them with $\boldsymbol{u}_g^p$ and $\boldsymbol{u}_l^p$, respectively, by the following equations:

$$\boldsymbol{u}_l^* = \begin{cases} \boldsymbol{u}_l^p, & \text{if } -r \leqslant \phi \leqslant 0, \\ \boldsymbol{u}_l', & \text{otherwise}, \end{cases}$$
$$\boldsymbol{u}_g^* = \begin{cases} \boldsymbol{u}_g^p, & \text{if } 0 \leqslant \phi \leqslant r, \\ \boldsymbol{u}_g', & \text{otherwise}, \end{cases} \tag{3}$$

where the distance $r = 2h$ with $h$ being the width of one cell and $\phi$ is the level-set function obtained in the above step of interface tracking.

Step 3: particle resampling. As the particles being advected, particles would move out or accumulate at the bands, leading to the number of particles in some cell of the bands less (or more) than $n$ (resp. $2n$) (the default $n = 8$). To address these

issues, we delete the particles outside of the bands or in cells with more than $2n$ particles, and add new particles to cells with less than $n$ particles.

*Octree-based Poisson solver.* In order to further speed up MultiFLIP, we propose to solve the variable coefficient Poisson equation on octrees. In the following, we first introduce the discretization of (2a). Then, we introduce how to add the surface tension term.

• Discretization. We construct an octree with refined grid cells near the gas-liquid interface according to the constructed level set function, as shown in Figure 1(f). Then, we discretize the variable coefficient Poisson equation of (2a) on the octree based on the scheme of Lossasso et al. [4]. By the divergence theorem, for a cell $i$, the left term of (2a) is discretized as follows:

$$V_i \nabla \cdot \frac{1}{\rho} \nabla p = \sum_k A_{i,k} \frac{1}{\rho_{i,k}} \frac{p_i - p_k}{\Delta_{i,k}}, \qquad (4)$$

where $V_i$ is the volume of $i$ cell; $A_{i,k}$ and $\Delta_{i,k}$ are the area and distance between $i$ and $k$ cell; $p_i$ and $p_k$ denote the pressure stored in the centers of $i$ cell and its neighbor cells, respectively. These variables are illustrated in the left figure of Figure 1(g) for 2D case. Specially, $\rho_{i,k}$ is set to $\rho_g$ (resp. $\rho_l$) of the gas (resp. liquid) density, if both $i$ and $k$ cells are in the gas (liquid) domain. Otherwise, the two cells must be separated by the interface. In this case, $\rho_{i,k}$ is set to $\theta\rho_l + (1-\theta)\rho_g$, where $\theta$ is computed according to the location of interface as illustrated in Figure 1(h).

For the liquid or gas domain, we discretize the divergence of $i$ cell in the right term of (2a) by

$$V_i \nabla \cdot \boldsymbol{u}^* = \sum_k A_{i,k} (\boldsymbol{u}^* \cdot \boldsymbol{n}_{i,k}), \qquad (5)$$

where $\boldsymbol{u}^* = \boldsymbol{u}_g^*$ for the gas or $\boldsymbol{u}_l^*$ for the liquid, and $\boldsymbol{n}_{i,k}$ is the outer-pointing normal of face $A_{i,k}$ as shown in Figure 1(g). For the domain occupied by both the gas and liquid, we use the same scheme as MultiFlIP to discretize the divergence.

• Surface tension. In order to simulate the surface tension, we add $\frac{1}{\rho_{i,k}} \frac{\sigma\kappa}{\Delta_{i,k}^2}$ to the right side of (2a) like MultiFLIP. $\sigma$ is the surface tension coefficient for the interface and $\kappa$ is the mean curvature of the interface. Since $\kappa$ only has non-zero values on the interface, $\frac{1}{\rho_{i,k}} \frac{\sigma\kappa}{\Delta_{i,k}^2}$ only affects the two cells crossed by the interface with $\rho_{i,k} = \theta\rho_l + (1-\theta)\rho_g$, as shown in Figure 1(h).

Combining all these terms into one equation, we get a sparse positive semi-definite linear equation, which is solved by PCG.

*Results.* The performance data of our experiments, including gas and liquid particle numbers, runtimes and memory cost, can be founded in Figure 1(i). Please see our results in the attached video.

*Conclusion and future work.* We have introduced two techniques to improve the efficiency of MultiFLIP. Our experiments have showed that the use of two narrow bands to tracking gas-liquid interface can significantly reduce the number of particles while keeping simulation quality. On the other hand, the use of octree structures greatly reduces the unknowns of the variable coefficient Poisson equation, thus speedup the projection step. By the two techniques, $4 \sim 6$x memory reduction and time speedup have been gained over the original MultiFLIP. In future work, we consider to use more advanced adaptive Poisson solvers, such as the power diagram method by Aanjaneya et al. [7] and GPU-friendly data structures in Hoetzlein [8].

**Acknowledgements** The work was supported by National Key R&D Program of China (Grant No. 2017YFB1002701), Macao FDCT Fund (Grant Nos. 068/2015/A2, 136/2014/A3), National Natural Science Foundation of China (NSFC) (Grant Nos. 61672502, 61632003 ,61502109), UM Research Fund (Grant No. MYRG2014-00139-FST), and Natural Science Foundation of Guangdong Province (Grant No. 2016A030310342).

**Supporting information** Videos and other supplemental documents. The supporting information is available online at info.scichina.com and link.springer.com. The supporting materials are published as submitted, without typesetting or editing. The responsibility for scientific accuracy and content remains entirely with the authors.

## References

1 Boyd L, Bridson R. MultiFLIP for energetic two-phase fluid simulation. ACM Trans Graph, 2012, 31: 1–12
2 Zhu Y N, Bridson R. Animating sand as a fluid. ACM Trans Graph, 2005, 24: 965–972
3 Ferstl F, Ando R, Wojtan C, et al. Narrow band FLIP for liquid simulations. Comput Graph Forum, 2016, 35: 225–232
4 Losasso F, Gibou F, Fedkiw R. Simulating water and smoke with an octree data structure. ACM Trans Graph, 2004, 23: 457–462
5 Bridson R. Fluid Simulation for Computer Graphics. 2nd ed. Thames: Taylor & Francis, 2015
6 Liu X D, Fedkiw R P, Kang M. A boundary condition capturing method for poisson's equation on irregular domains. J Comput Phys, 2000, 160: 151–178
7 Aanjaneya M, Gao M, Liu H X, et al. Power diagrams and sparse paged grids for high resolution adaptive liquids. ACM Trans Graph, 2017, 36: 1–12
8 Hoetzlein R K. GVDB: raytracing sparse voxel database structures on the GPU. In: Proceedings of High Performance Graphics, Dublin, 2016. 109–117